

# EVIDENCE-GATED LLM PRIORS FOR MULTI-OBJECTIVE BAYESIAN OPTIMIZATION

**Jiangyu Chen\*** **Banyi\***

State Key Laboratory for Novel Software Technology, Nanjing University  
jianyuchen@smail.nju.edu.cn

**Tianfan Fu†**

State Key Laboratory for Novel Software Technology, Nanjing University  
futianfan@nju.edu.cn

## ABSTRACT

Large language models (LLMs) are increasingly used as heuristic advisors for black-box optimization, yet their suggestions and self-reported confidence are not necessarily calibrated to downstream objective values. This issue becomes more pronounced in multi-objective Bayesian optimization, where different objectives may require different expert knowledge and where an LLM expert can be useful for one objective but misleading for another.

We study how to use LLM-generated expert priors in discrete multi-objective Bayesian optimization without blindly trusting them. We propose an objective-wise reputation-market mechanism that treats each expert-objective pair as a falsifiable prior source. Expert weights are updated online from observed objective feedback, discounted over time, and gated by market-level trust. We then introduce a decoupled counterfactual gate that can use the LLM prior without confidence, use it with confidence, or abstain from the LLM prior entirely.

Across controlled synthetic stress tests and three molecule optimization benchmarks with Qwen3.6-Flash-generated expert priors, we find that dynamic objective-wise calibration improves robustness over fixed LLM priors. However, raw LLM confidence is not reliably beneficial: on ESOL, confidence is positively correlated with prediction error; on FreeSolv, confidence can help; and on Lipophilicity, ignoring confidence remains strongest. Our fixed three-arm counterfactual gate improves over the first counterfactual variant on ESOL and FreeSolv, while an attempted margin portfolio exposes a useful negative result: margin selection should be acquisition-aware rather than based only on one-step prior error.

## 1 INTRODUCTION

Bayesian optimization (BO) is a standard tool for expensive black-box optimization, where each evaluation may require a laboratory experiment, a simulation, or a costly model call Jones et al. (1998); Frazier (2018). Its sample efficiency depends heavily on the surrogate model and the acquisition function. This is precisely where large language models (LLMs) are tempting: they contain broad semantic and scientific knowledge, can reason over structured descriptions such as molecules or prompts, and can often provide plausible qualitative judgments before any task-specific data are observed.

Recent LLM-BO work has explored this opportunity in several directions. Some methods use LLMs as optimizers or proposal engines, asking them to generate candidates, prompts, kernels, or acquisition functions. Others use BO as an outer-loop tool for tuning LLM systems, such as prompt selection, checkpoint merging, model fusion, compression, or data-mixture design. These are

\*Both authors contributed equally to this research.

†Corresponding author.

important directions, but they leave a basic question underexplored: if an LLM is not the optimizer itself, can it still serve as a useful Bayesian prior inside BO?

Treating LLM output as a prior is attractive because even an imperfect prior can accelerate search in the low-data regime. It is also risky. LLM scores are not calibrated observations. A persona can be useful for one objective but misleading for another; several personas can make correlated mistakes; and self-reported confidence may express linguistic certainty rather than statistical reliability. In multi-objective BO, these failure modes are especially visible: a single global trust weight can hide objective-specific expertise, while a fixed confidence rule can help one objective and hurt another.

This paper studies LLMs as uncertain, falsifiable, objective-wise Bayesian priors. Our premise is simple: an LLM prior should influence BO only to the extent that it earns trust from observed objective feedback. It should be updated separately for each expert and objective, its confidence should be treated as another uncertain signal, and the optimizer should be able to abstain from the prior when evidence contradicts it.

We instantiate this idea in discrete multi-objective BO. Multiple LLM expert roles produce objective-wise prior scores and self-reported confidence values for every candidate. The BO loop fits residual Gaussian-process surrogates after subtracting an aggregated LLM prior. Expert-objective trust is updated online through a reputation market, and a decoupled counterfactual gate decides whether to use the prior without confidence, use it with confidence, or drop the prior entirely. Because the expert market evolves deterministically, the gate can replay counterfactual confidence decisions after each observation instead of waiting for high-variance long-horizon rewards.

**Contributions.** Our contributions are:

1. We formulate LLM-generated expert predictions as residual priors for multi-objective BO, with trust indexed by both expert and objective.
2. We introduce CF-V2, a compact evidence-gated algorithm combining an objective-wise reputation market with decoupled counterfactual gates for prior use and confidence-weighted updates.
3. We show empirically that self-reported LLM confidence is not a reliable probability-like signal: it can help, hurt, or matter only in specific algorithmic phases.
4. We evaluate on controlled synthetic stress tests and three molecule optimization benchmarks, showing gains on ESOL and FreeSolv, a clear limitation on Lipophilicity, and a negative result for one-step prior-error-based margin selection.

## 2 RELATED WORK

**Bayesian optimization and multi-objective BO.** Bayesian optimization originated as a sample-efficient framework for expensive black-box functions, with expected improvement and Gaussian-process surrogates forming a classical foundation Jones et al. (1998); Frazier (2018). Multi-objective BO extends this setting to competing objectives. ParEGO reduces multi-objective optimization to randomized scalarized subproblems Knowles (2006), while hypervolume-based methods such as qEHVI and qNEHVI directly optimize expected hypervolume improvement in parallel and noisy settings Daulton et al. (2020; 2021). Our experiments use these methods as strong baselines where available, implemented through BoTorch Balandat et al. (2020).

**LLMs for black-box optimization.** Recent work explores using LLMs inside optimization loops. LLAMBO frames BO problems in natural language and uses LLMs to propose and evaluate candidate solutions conditioned on historical evaluations Liu et al. (2024). InstructZero uses BO to optimize soft prompts that generate instructions for black-box LLMs Chen et al. (2023). Prompt-optimization methods similarly treat LLM behavior as a black-box objective. Our work differs in focus: rather than using an LLM as the optimizer or optimizing prompts for LLM performance, we use LLMs as uncertain expert prior sources inside a MOBO loop and learn how much to trust them from observed objective feedback.

This distinction matters because an LLM prior can be partially useful even when it is not accurate enough to choose candidates directly. In our setting, the LLM does not replace the acquisition

function; it provides structured prior functions that are continuously falsified by observations. The algorithmic question is therefore not only how to ask the LLM for better suggestions, but how to attenuate, reweight, or drop those suggestions when the BO evidence disagrees.

**Recent LLM–BO design patterns.** The 2024–2026 literature shows several ways to combine language models and BO. One line uses LLMs to improve BO itself: LLAMBO converts BO histories into language for candidate generation Liu et al. (2024); BOPRO uses BO-style exploration and exploitation to guide test-time LLM search BOPRO; FunBO searches over acquisition-function code generated by LLMs FunBO; BAKER uses LLM mutation and crossover operators for kernel design CAKE; LMABO selects acquisition functions from the BO state LMABO; LGBO injects LLM preferences into scientific-discovery BO loops LGBO; and BOLT uses LLMs for scalable multi-task BO initialization BOLT. A second line uses BO as a tool for optimizing LLM systems, including model fusion Model Fusion, low-rank compression Ji et al. (2024), prompt selection Schneider et al. (2025), checkpoint merging Liu et al. (2025), and data-mixture optimization Data Mixture Optimization. A third line uses generative sequence models as scientific priors for BO, for example in antibody design CloneBO.

Our work is closest to the first and third lines, but differs in the role assigned to the LLM. We do not ask the LLM to write the acquisition function, choose the kernel, or directly generate the next candidate. Instead, we turn multiple LLM personas into objective-wise prior functions and make their influence falsifiable inside the BO loop.

**Confidence calibration and verbalized uncertainty.** Confidence calibration studies whether predicted confidence corresponds to empirical correctness Guo et al. (2017). LLMs complicate this problem because uncertainty may be expressed verbally rather than through logits. Prior work shows that language models can be trained or prompted to express uncertainty in words Lin et al. (2022), and that models may contain internal signals about what they know even when their expressed answers are unreliable Kadavath et al. (2022). Our results complement this literature by studying the downstream optimization consequences of self-reported LLM confidence. We find that confidence can help, hurt, or be useful only in specific algorithmic phases.

We therefore treat confidence as an input whose role must itself be learned. This is different from post-hoc calibration on a fixed supervised benchmark: the consequence of miscalibration here is sequential, because an overconfident wrong prior can change which candidates are evaluated next and thus change the future training set of the surrogate.

**Prediction with expert advice.** Our reputation-market mechanism is related to online learning with expert advice, where expert weights are updated based on observed losses Freund & Schapire (1997); Cesa-Bianchi & Lugosi (2006). Unlike standard expert-advice settings, our experts produce objective-wise prior functions used inside a Bayesian optimization surrogate, and the feedback is only observed for sequentially sampled candidates. This motivates expert-objective capital, temporal discounting, and market-level trust gates rather than a single global expert weight.

The counterfactual gates also use an expert-advice perspective, but in a deterministic replay form. Because both confidence-on and confidence-off updates can be replayed after observing a new objective value, the gate receives full-information feedback rather than bandit feedback. This lets the method make phase decisions from internal counterfactual evidence without waiting for long-horizon hypervolume changes.

### 3 PROBLEM SETTING

We consider discrete multi-objective black-box optimization. Let the candidate set be

$$\mathcal{X} = \{x_1, \dots, x_N\}.$$

Each candidate has an unknown objective vector

$$\mathbf{f}(x) = (f_1(x), \dots, f_m(x)).$$

The optimizer begins with a small initial design and sequentially selects candidates to evaluate. The goal is to maximize multi-objective performance under a limited evaluation budget. In our

experiments,  $m = 2$  and we measure performance by final hypervolume, AUC hypervolume, and best objective-sum.

We assume access to a set of LLM/expert priors. For each candidate  $x$ , expert  $e$ , and objective  $j$ , the expert provider returns a predicted normalized objective score  $\mu_{ej}(x)$  and a self-reported confidence value  $c_{ej}(x)$ . Both may be misspecified. The optimizer must decide which experts to trust, for which objectives, and whether self-reported confidence should influence prior aggregation or online expert-weight updates.

## 4 METHOD

### 4.1 LLM EXPERTS AS OBJECTIVE-WISE PRIORS

We instantiate multiple expert roles, such as solubility-oriented, drug-likeness-oriented, or balanced ADMET experts. Each expert returns objective-wise scores and confidence values. These predictions are cached and used as prior information during BO.

Given trust weights  $\alpha_{ej}$ , the aggregated prior for objective  $j$  is

$$p_j(x) = \frac{\sum_e \alpha_{ej} \tilde{c}_{ej}(x) \mu_{ej}(x)}{\sum_e \alpha_{ej} \tilde{c}_{ej}(x)},$$

where  $\tilde{c}_{ej}(x)$  is the effective confidence after optional calibration or gating. The surrogate model is fit to residuals:

$$f_j(x) = p_j(x) + r_j(x).$$

This lets the optimizer use LLM prior structure while still correcting it with observed objective values.

### 4.2 OBJECTIVE-WISE REPUTATION MARKET

The main strategy maintains a capital value for each expert-objective pair:

$$K_{ej}.$$

At an observed point  $(x_t, \mathbf{y}_t)$ , we compute standardized error

$$\epsilon_{ej,t} = \frac{|\mu_{ej}(x_t) - y_{j,t}|}{s_{j,t}},$$

where  $s_{j,t}$  is a running objective scale. A soft success score is

$$q_{ej,t} = \exp(-\frac{1}{2}\epsilon_{ej,t}^2).$$

The capital update uses a proper-score-like reward:

$$R_{ej,t} = \text{clip}(0.5 - 0.5\epsilon_{ej,t}^2, -2.0, 0.75),$$

$$K_{ej,t+1} = (1 - \lambda)K_{ej,t} + \eta \tilde{c}_{ej}(x_t) R_{ej,t}.$$

Capital is converted into relative expert weights through a temperature-controlled softmax across experts. A market-level trust gate shrinks all prior weights when the expert market has low absolute reputation.

### 4.3 RESIDUAL SURROGATE AND ACQUISITION

Given the current prior  $p_{j,t}(x)$ , we fit a Gaussian-process residual surrogate to

$$r_{j,\tau} = y_{j,\tau} - p_{j,t}(x_\tau).$$

The posterior prediction for objective  $j$  is reconstructed as

$$\hat{f}_{j,t}(x) = p_{j,t}(x) + m_{j,t}^r(x),$$

where  $m_{j,t}^r$  is the residual posterior mean. We use a randomized scalarized UCB rule for the residual-prior methods:

$$A_t(x) = \sum_{j=1}^m w_{j,t} \left( \hat{f}_{j,t}(x) + \beta_t s_{j,t}^r(x) \right) + \gamma(1 - \bar{\alpha}_t) \sum_{j=1}^m w_{j,t} D_j(x).$$

Here  $w_t$  is a random objective weight vector,  $s_{j,t}^r$  is residual posterior uncertainty,  $D_j(x)$  is expert disagreement for objective  $j$ ,  $\bar{\alpha}_t$  is average market trust,  $\beta_t = 1 + 1.25(1 - \bar{\alpha}_t)$ , and  $\gamma = 0.30$ . When expert trust is low, the method therefore explores more and gives additional value to candidates where experts disagree.

#### 4.4 DIAGNOSTIC CONFIDENCE VARIANTS

We do not assume that LLM confidence is calibrated. Before fixing the final algorithm, we evaluate raw confidence, no confidence, softened confidence, prior-only confidence, update-only confidence, and adaptive confidence gates as diagnostic variants.

For one adaptive baseline, the optimizer tracks whether confidence predicts expert success. For each objective, it maintains an online pooled correlation between reported confidence and soft success:

$$\rho_j = \text{CORR}(c_{ej,t}, q_{ej,t}).$$

The gate is

$$g_j = \sigma(a_\rho(\rho_j - \tau_\rho)).$$

When the correlation is non-positive or insufficiently supported, the gate closes. Effective confidence is

$$\tilde{c}_{ej}(x) = 1 + g_j(c_{ej}(x) - 1).$$

Thus  $g_j = 0$  ignores confidence and  $g_j = 1$  uses raw confidence.

Confidence can influence two parts of the algorithm:

1. prior aggregation, which changes the prior score used to rank candidates;
2. reputation updates, which changes how experts are rewarded or punished.

We therefore include fixed phase variants in the ablation. These variants are not the final method; they are used to expose when confidence is useful in prior aggregation, reputation updates, both, or neither.

#### 4.5 DECOUPLED COUNTERFACTUAL GATE

Our final algorithm, denoted CF-V2, keeps the reputation-market update but replaces a single confidence gate with two counterfactual decisions. This is the key difference from earlier confidence-phase variants: CF-V2 does not merely decide whether to multiply by self-reported confidence. It asks two separate evidence questions: whether the LLM prior should enter the surrogate at all, and whether confidence should scale future expert-credit updates. The prior gate controls how the aggregated LLM prior enters the residual surrogate. For each objective  $j$ , it compares three prior actions:

$$a \in \{\text{no\_conf}, \text{conf}, \text{drop}\}.$$

The first action aggregates expert priors with confidence set to one, the second uses reported confidence, and the third sets the prior contribution to zero. For action  $a$ , define the historical residuals

$$r_{j,\tau}^{(a)} = y_{j,\tau} - p_j^{(a)}(x_\tau),$$

and score them with a fixed-kernel GP marginal likelihood

$$S_{j,t}(a) = \frac{1}{t} \log p(r_{j,1:t}^{(a)} | \mathcal{X}_t^{\text{obs}}).$$

The prior-arm logits are relative to the conservative no-confidence arm:

$$\ell_{j,t}(a) = \eta_p(S_{j,t}(a) - S_{j,t}(\text{no\_conf}) - \Delta_a),$$

where  $\Delta_{\text{no\_conf}} = \Delta_{\text{conf}} = 0$  and  $\Delta_{\text{drop}} = 0.05$ . Probabilities are shrunk toward the no-confidence arm when evidence is limited. With  $n_t$  observations and count scale  $\kappa_0$ , the shrinkage factor is

$$\kappa_t = \sqrt{\frac{n_t}{n_t + \kappa_0}},$$

and the prior-arm probabilities are

$$\pi_{j,t}^p = (1 - \kappa_t) \mathbf{e}_{\text{no\_conf}} + \kappa_t \text{softmax}_a(\ell_{j,t}(a)).$$

The effective prior used by the residual surrogate is the arm mixture

$$p_{j,t}(x) = \pi_{j,t}^p(\text{no\_conf}) p_{j,t}^{(\text{no\_conf})}(x) + \pi_{j,t}^p(\text{conf}) p_{j,t}^{(\text{conf})}(x),$$

because the drop arm contributes zero prior. This makes prior abstention explicit rather than implicit in a small expert weight. This explicit drop action is the crucial distinction in CF-V2: when the LLM prior is systematically wrong, the residual surrogate can fall back toward ordinary GP-based BO instead of being forced to explain away a biased prior.

The update gate controls whether confidence should scale expert rewards. It maintains two deterministic shadow markets, one that replays updates without confidence and one that replays them with confidence. After observing  $\mathbf{y}_t$ , both shadow markets predict the current point, and we compute

$$L_{j,t}^u(g) = |y_{j,t} - p_j^{(g)}(x_t)| / s_{j,t}, \quad g \in \{0, 1\}.$$

The update gate is then updated by full-information Hedge. In implementation we center the two losses before the logit update, which is algebraically equivalent for the resulting softmax probabilities but improves numerical stability:

$$\bar{L}_{j,t}^u(g) = L_{j,t}^u(g) - \frac{1}{2} \sum_{g' \in \{0,1\}} L_{j,t}^u(g'),$$

$$\pi_{j,t+1}^u(g) \propto \pi_{j,t}^u(g) \exp(-\eta_u \bar{L}_{j,t}^u(g)).$$

Using  $L^u$  instead of  $\bar{L}^u$  gives the same softmax probabilities, since centering subtracts the same constant from both arms within an objective. As with the prior gate, early update-gate probabilities are shrunk toward a neutral two-arm distribution until the minimum evidence count is reached. This separates prior abstention from confidence-weighted reputation learning while keeping the algorithm deterministic and reproducible.

## 4.6 ALGORITHM SUMMARY

**Main loop.** Once the random seed, initial design, and cached LLM priors are fixed, CF-V2 is deterministic. The loop is:

1. Generate or load cached LLM expert predictions  $\mu_{ej}(x)$  and confidence values  $c_{ej}(x)$  for all candidates.
2. Initialize BO with a small random design and evaluate true objectives.
3. At iteration  $t$ , update expert-objective capital values and the update-gate shadow markets from the newest observed prediction errors.
4. Replay the three prior arms on the observed history and update the counterfactual prior gate.
5. Aggregate the LLM prior through the three-arm prior mixture and fit a residual surrogate.
6. Select the next candidate by the scalarized residual-UCB acquisition above.
7. Repeat until the evaluation budget is exhausted.

The important design choice is that all expert trust is indexed by both expert and objective. This allows the optimizer to learn that a role can be useful for one objective while being misleading for another.

## 5 EXPERIMENTS

### 5.1 SYNTHETIC STRESS TESTS

We construct controlled two-objective synthetic benchmarks with expert failure modes: all experts useful, all experts misleading, objective-wise specialization, overconfident bad experts, noisy experts, and correlated bad experts. These tests isolate whether the method can exploit useful priors and resist harmful priors.

Table 1: Fixed CF-V2 hyperparameters used for the main molecule experiments.

Component	Hyperparameter	Value
Reputation market	reward step $\eta$	0.45
Reputation market	discount $\lambda$	0.015
Reputation market	capital softmax temperature	0.55
Market trust	threshold / slope	0.48 / 7.0
Prior gate	evidence score	GP marginal likelihood
Prior gate	$\eta_p$ / min updates / count scale	1.0 / 4 / 4.0
Prior gate	$\Delta_{\text{drop}}$	0.05
Prior evidence GP	noise / lengthscale	0.05 / median distance
Update gate	$\eta_u$	1.0
Acquisition	$\beta_t$ / disagreement $\gamma$	$1 + 1.25(1 - \bar{\alpha}_t) / 0.30$

Table 2: Molecule benchmark setup.

Dataset	Pool size	Initial design	Budget	Seeds
ESOL	100	8	30	10
FreeSolv	100	8	16	10
Lipophilicity	150	8	16	10

## 5.2 MOLECULE OPTIMIZATION BENCHMARKS

We evaluate on ESOL, FreeSolv, and Lipophilicity candidate pools. For each dataset, Qwen3.6-Flash-generated expert priors are cached before optimization so all methods share the same LLM prior data. The main metric is final hypervolume under a limited evaluation budget. We additionally run ESOL backend diagnostics with Qwen3.7-Max and DeepSeek-V4-Pro.

## 5.3 BASELINES

We compare against random search, vanilla MOBO, fixed LLM priors, EMA reliability, beta reliability, ParEGO, qLogEHVI, qLogNEHVI, fixed confidence-phase variants, and earlier counterfactual-gate variants.

**Implementation details.** All molecule experiments use cached LLM priors so that methods differ only in how they use the same expert information. Hypervolume is computed on normalized objectives with the origin as the reference point. For calibrated expert-prior methods, the residual surrogate is fit after subtracting the current aggregated expert prior. CF-V2 uses the three-arm prior gate above with fixed  $\Delta_{\text{drop}} = 0.05$ ; the drop-margin portfolio is reported only as a diagnostic ablation.

# 6 RESULTS

## 6.1 MAIN MOLECULE RESULTS

CF-V2 gives the best final hypervolume on ESOL and FreeSolv among the compared methods in Table 3. On ESOL, it improves over raw reputation-market weighting, fixed LLM priors, vanilla MOBO, and qLogNEHVI, while also achieving the best AUC hypervolume. On FreeSolv, the gain over vanilla MOBO and fixed priors is larger, suggesting that online expert-objective calibration is most useful when the cached LLM priors contain task-relevant signal but are not reliable enough to use statically.

Lipophilicity is the main counterexample. CF-V2 remains competitive with vanilla MOBO and raw reputation-market weighting, but qLogNEHVI and the no-confidence phase diagnostic are stronger. We treat this as evidence against a universal confidence-using story: for this dataset, the safest action is often to ignore LLM confidence and rely more heavily on the surrogate.

Table 3: Main molecule optimization results. Final hypervolume is reported as mean  $\pm$  standard deviation over seeds.

Dataset	Method	Final HV	AUC HV	Best sum
ESOL	Ours (CF-V2)	0.7561 $\pm$ 0.0042	0.7108	1.4805
ESOL	Rep. Market (raw)	0.7484 $\pm$ 0.0101	0.6982	1.4805
ESOL	qLogNEHVI	0.7431 $\pm$ 0.0209	0.6966	1.4772
ESOL	ParEGO	0.7119 $\pm$ 0.0406	0.6729	1.4610
ESOL	Vanilla MOBO	0.7359 $\pm$ 0.0325	0.6903	1.4756
ESOL	Fixed LLM Prior	0.7417 $\pm$ 0.0169	0.6936	1.4805
ESOL	Random	0.7025 $\pm$ 0.0307	0.6637	1.4601
FreeSolv	Ours (CF-V2)	0.5798 $\pm$ 0.0680	0.4664	1.3243
FreeSolv	Rep. Market (raw)	0.5702 $\pm$ 0.0681	0.4523	1.3195
FreeSolv	qLogNEHVI	0.5370 $\pm$ 0.1038	0.4106	1.3055
FreeSolv	Vanilla MOBO	0.5033 $\pm$ 0.1245	0.3825	1.2868
FreeSolv	Fixed LLM Prior	0.4804 $\pm$ 0.0510	0.4128	1.2950
FreeSolv	Random	0.3062 $\pm$ 0.0868	0.2942	1.0968
Lipophilicity	Ours (CF-V2)	0.8953 $\pm$ 0.0383	0.8554	1.8668
Lipophilicity	Rep. Market (raw)	0.8958 $\pm$ 0.0433	0.8710	1.8781
Lipophilicity	qLogNEHVI	0.9042 $\pm$ 0.0303	0.8723	1.8996
Lipophilicity	Vanilla MOBO	0.8954 $\pm$ 0.0280	0.8690	1.8740
Lipophilicity	Fixed LLM Prior	0.8878 $\pm$ 0.0503	0.8648	1.8788
Lipophilicity	Random	0.8688 $\pm$ 0.0504	0.8457	1.8584

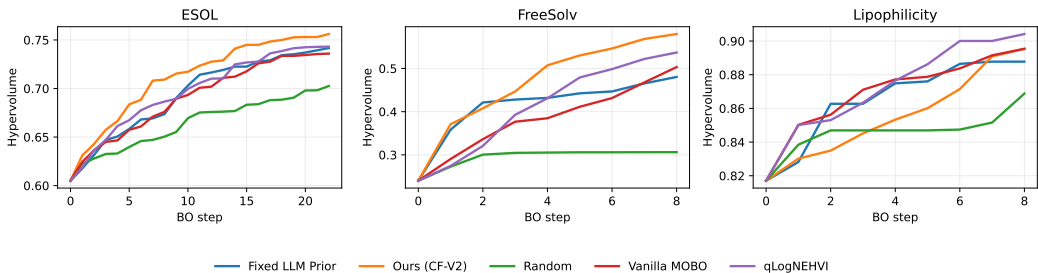


Figure 1: Mean hypervolume curves on molecule tasks.

Table 4: Synthetic stress-test results. Dynamic reputation weighting improves over fixed LLM priors across controlled prior-misspecification scenarios.

Scenario	Rep. market	Fixed	Vanilla	Random
All useful	<b>0.4805</b>	0.4791	0.4359	0.3510
All misleading	0.4262	0.3922	<b>0.4359</b>	0.3510
Objective-specialized	<b>0.4791</b>	0.4663	0.4359	0.3510
Overconfident bad	<b>0.4750</b>	0.4640	0.4359	0.3510
Noisy experts	<b>0.4715</b>	0.4247	0.4359	0.3510
Correlated bad experts	<b>0.4586</b>	0.4235	0.4359	0.3510

Table 5: Confidence-phase ablation on molecule tasks. The best phase differs across datasets.

Dataset	Raw	No conf.	Prior only	Adaptive	Adapt. prior	Adapt. update
ESOL	0.7490	0.7550	0.7535	0.7520	0.7566	0.7471
FreeSolv	0.5702	0.5440	0.5702	0.5589	0.5390	0.5616
Lipophilicity	0.8958	0.9081	0.8888	0.9014	0.9025	0.9054

Table 6: Core algorithm ablation. CF-V2 is the fixed three-arm counterfactual gate used as the main method; the margin portfolio is retained only as a diagnostic variant.

Dataset	Best fixed phase	Best fixed HV	CF-V1	CF-V2	Margin portfolio
ESOL	Adaptive prior	0.7566	0.7448	0.7561	0.7520
FreeSolv	Prior only	0.5702	0.5493	0.5798	0.5444
Lipophilicity	No conf.	0.9081	0.8940	0.8953	0.8892

## 6.2 SYNTHETIC STRESS TESTS

Synthetic stress tests show that dynamic reputation weighting improves over fixed LLM priors across controlled prior-misspecification scenarios. In the all-bad setting, reputation-market remains below vanilla BO, showing that fallback is not yet perfectly lossless, but it substantially reduces the damage of fixed misleading priors.

## 6.3 CONFIDENCE CALIBRATION AND PHASE ABLATION

On ESOL, Qwen3.6-Flash confidence is positively correlated with absolute prediction error. This motivates treating confidence as another uncertain signal rather than a calibrated probability.

The phase ablation in Table 5 shows why a single global rule for LLM confidence is brittle. ESOL prefers adaptive prior confidence, FreeSolv prefers prior-only or raw confidence, and Lipophilicity prefers no confidence. This objective- and dataset-level heterogeneity motivates the decoupled design of CF-V2 rather than a fixed confidence multiplier.

Table 6 compares the compressed main algorithm with important development variants. CF-V2 improves over the first counterfactual gate on ESOL and FreeSolv, and it is close to the best fixed phase on ESOL. It does not match the no-confidence diagnostic on Lipophilicity, which again supports a cautious interpretation: the method improves robustness, but abstention is not yet perfect.

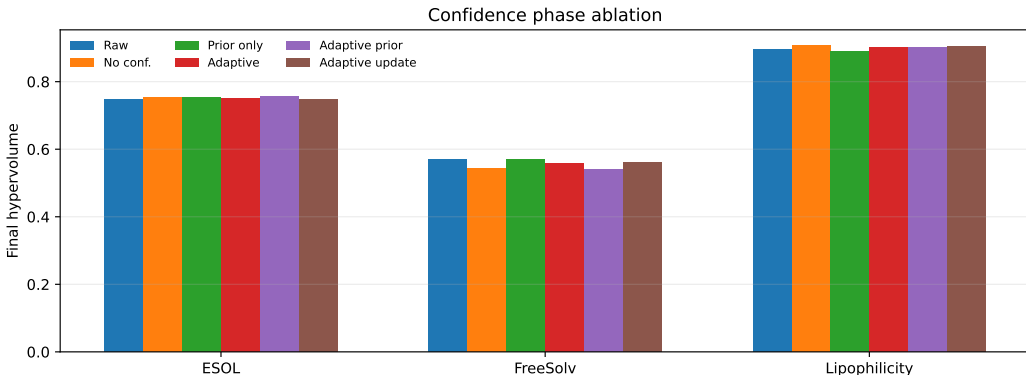


Figure 2: Confidence phase ablation. The best way to use confidence differs by dataset.

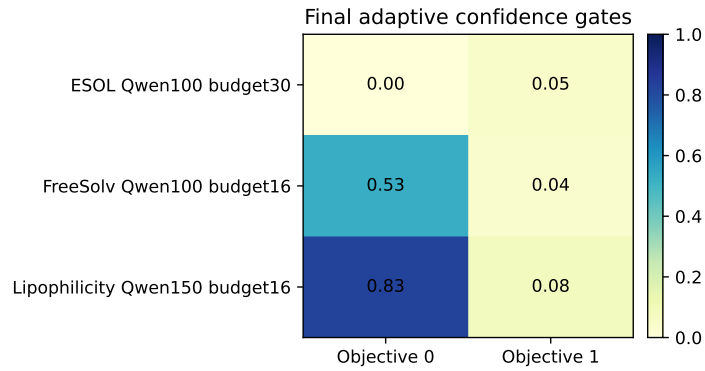


Figure 3: Final adaptive confidence gates by objective. Confidence is often useful for one objective and weak or harmful for another.

#### 6.4 MECHANISM DIAGNOSTICS

The trajectory plots in Figure 4 expose the causal state of the prior gate rather than only reporting final hypervolume. The reputation heatmaps in Figure 5 provide the complementary view: expert roles separate by objective over time, which is the behavior required for multi-objective LLM priors to be useful rather than merely decorative.

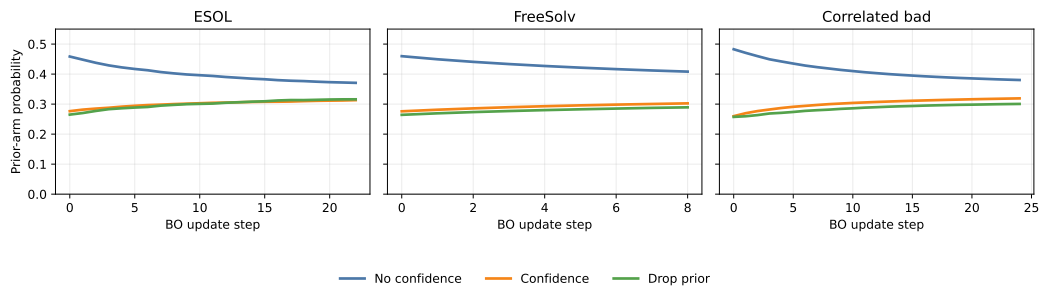


Figure 4: Causal trajectory of the CF-V2prior gate. Each curve shows the mean softmax probability of one prior arm, averaged over seeds and objectives. The gate starts near the conservative no-confidence arm and reallocates probability mass as counterfactual GP evidence accumulates.

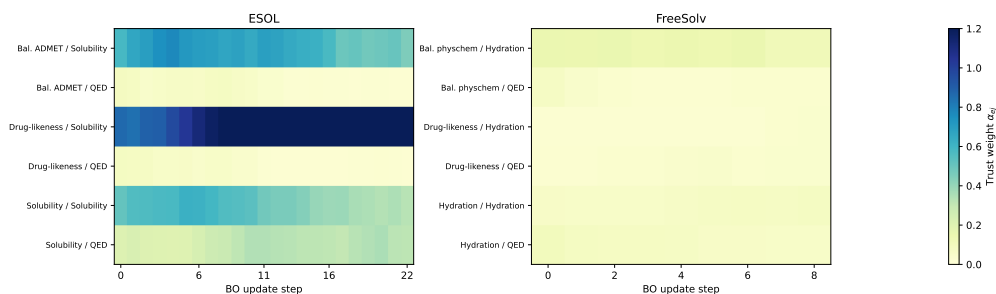


Figure 5: Objective-wise reputation-market dynamics. Rows correspond to LLM expert roles crossed with objectives; columns are BO update steps. The heatmap shows that expert trust evolves differently across objectives rather than collapsing to one global LLM weight.

## 6.5 ORACLE PHASE DIAGNOSTIC

The oracle phase diagnostic in Table 7 estimates the upside of choosing the best confidence phase per seed after the fact. The gap is small on ESOL, larger on FreeSolv, and moderate on Lipophilicity. Thus, online phase selection is not necessary for a coherent main algorithm, but it remains a plausible source of future improvement.

The backend diagnostic in Table 8 records the failed first attempt at automatic drop-margin selection. A replay-loss margin portfolio is not consistently better than a fixed margin across Qwen3.6-Flash, Qwen3.7-Max, and DeepSeek-V4-Pro priors. This is a useful negative result: choosing  $\Delta_{\text{drop}}$  from one-step prior error alone can prefer locally accurate but overly conservative priors, whereas BO performance depends on acquisition behavior and exploration.

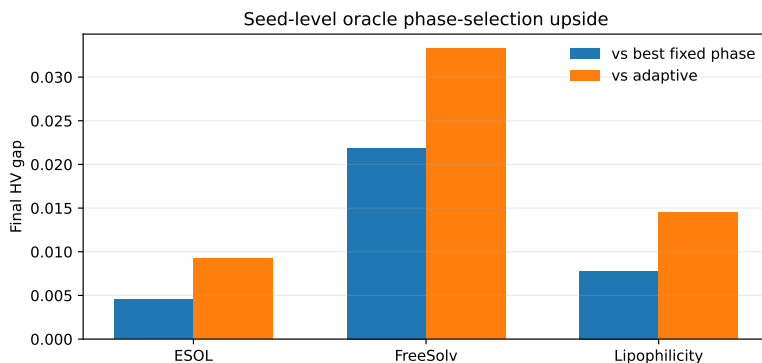


Figure 6: Seed-level oracle phase-selection upside. The gap estimates the potential value of a future online meta-gate.

Table 7: Oracle phase-selection diagnostic. Seed-level oracle values estimate the upside of an online meta-gate.

Dataset	Best fixed phase	Best fixed HV	Seed oracle HV	Oracle gap	Gap vs adaptive
ESOL	Adaptive prior	0.7566	0.7612	0.0046	0.0092
FreeSolv	Prior only	0.5702	0.5921	0.0219	0.0333
Lipophilicity	No conf.	0.9081	0.9159	0.0078	0.0145

Table 8: Model-backend diagnostic for drop-margin selection. The first margin-portfolio attempt does not consistently replace a fixed margin.

Setting	Best fixed margin	Margin portfolio
ESOL / Qwen3.6-Flash	0.7561	0.7520
ESOL / Qwen3.7-Max	0.7507	0.7480
ESOL / DeepSeek-V4-Pro	0.7500	0.7514

## 7 DISCUSSION

The central result is not that LLM confidence always helps BO. A more defensible claim is that LLM priors and LLM confidence are both uncertain signals. BO should calibrate them online, objective by objective, and should be able to attenuate or ignore them when evidence contradicts them.

The multi-objective setting is essential because it exposes role-objective mismatch. An expert can be correct for one objective and wrong for another. A global expert weight hides this structure. Our learned weights and gates repeatedly show objective-wise asymmetry.

The phase ablation suggests that confidence should not be treated as a single scalar modifier. Confidence can affect prior aggregation or expert updates, and these roles behave differently across tasks. CF-V2 operationalizes this observation by decoupling the prior and update decisions and by adding an explicit prior-abstention action.

The drop-margin portfolio experiment is an important negative result. It learns margins from one-step prior prediction error and therefore often prefers conservative margins. This can improve local prior accuracy but reduce BO hypervolume when aggressive prior abstention improves exploration or removes systematic bias. We therefore keep the fixed-margin CF-V2 algorithm as the main reproducible method and treat margin learning as future work.

## 8 LIMITATIONS

Current candidate pools are modest in size. Qwen3.6-Flash priors are studied most extensively, while Qwen3.7-Max and DeepSeek-V4-Pro checks are limited to ESOL. CF-V2 improves ESOL/Qwen3.6-Flash and FreeSolv but does not solve Lipophilicity, where no-confidence remains strongest. The margin portfolio is not yet a replacement for the fixed margin because prior-error rewards do not fully reflect downstream acquisition value.

## 9 REPRODUCIBILITY

The implementation contains scripts for data preparation, LLM prior generation, ablations, stress tests, and paper asset generation. The main paper assets are generated from completed experiment CSV files by:

```
uv run python scripts/build_paper_assets.py.
```

All tables in this draft are either generated under `paper/tables/` or derived from CSV files under `runs_molecule/` and `runs_pl/`. LLM priors are cached before BO runs, which makes optimization comparisons deterministic with respect to the generated prior cache.

## 10 FUTURE WORK

The next algorithmic step should be acquisition-aware margin selection. The current margin portfolio learns from one-step prior error, but  $\Delta_{\text{drop}}$  also controls exploration and bias removal. A better reward should combine prior fit with counterfactual acquisition rank or predicted hypervolume improvement.

## 11 CONCLUSION

We presented an evidence-gated approach to using LLM expert priors in multi-objective Bayesian optimization. The method treats each expert-objective pair as a falsifiable prior source, learns trust online from observed objective feedback, and uses a fixed three-arm counterfactual gate to use, discount, or drop the LLM prior. Experiments show that objective-wise reputation and counterfactual prior gating improve robustness on several molecule tasks, while confidence analysis shows that self-reported LLM confidence must itself be calibrated, gated, or ignored. These findings support a cautious view of LLMs in BO: useful as priors, but only when their influence is earned through evidence.

## REFERENCES

- Maximilian Balandat, Brian Karrer, Daniel R. Jiang, Samuel Daulton, Benjamin Letham, Andrew Gordon Wilson, and Eytan Bakshy. BoTorch: A framework for efficient monte-carlo bayesian optimization. In *Advances in Neural Information Processing Systems*, volume 33, pp. 21524–21538, 2020.
- BOLT. Scaling multi-task bayesian optimization with large language models. In *International Conference on Learning Representations*, 2026. URL <https://openreview.net/forum?id=ekmUkRYnkN>.
- BOPRO. Searching for optimal solutions with llms via bayesian optimization. In *International Conference on Learning Representations*, 2025. URL <https://openreview.net/forum?id=aVfDrl7xDV>.
- CAKE. Adaptive kernel design for bayesian optimization is a piece of cake with llms. In *Advances in Neural Information Processing Systems*, 2025. URL [https://papers.nips.cc/paper\\_files/paper/2025/hash/c03a2610bca2712b984b331fd4f7bb6f-Abstract-Conference.html](https://papers.nips.cc/paper_files/paper/2025/hash/c03a2610bca2712b984b331fd4f7bb6f-Abstract-Conference.html).
- Nicolò Cesa-Bianchi and Gábor Lugosi. *Prediction, Learning, and Games*. Cambridge University Press, 2006.
- Lichang Chen, Jiu-hai Chen, Tom Goldstein, Heng Huang, and Tianyi Zhou. InstructZero: Efficient instruction optimization for black-box large language models. In *International Conference on Machine Learning*, 2023.
- CloneBO. Bayesian optimization of antibodies informed by a generative model of evolving sequences. In *International Conference on Learning Representations*, 2025. URL [https://proceedings.iclr.cc/paper\\_files/paper/2025/hash/6cdd4ce9330025967ddled0bed3010f5-Abstract-Conference.html](https://proceedings.iclr.cc/paper_files/paper/2025/hash/6cdd4ce9330025967ddled0bed3010f5-Abstract-Conference.html).
- Data Mixture Optimization. Data mixture optimization: A multi-fidelity multi-scale bayesian framework. In *Advances in Neural Information Processing Systems*, 2025. URL <https://openreview.net/forum?id=Kvsa8ZXd0W>.
- Samuel Daulton, Maximilian Balandat, and Eytan Bakshy. Differentiable expected hypervolume improvement for parallel multi-objective bayesian optimization. In *Advances in Neural Information Processing Systems*, volume 33, pp. 9851–9864, 2020.

- Samuel Daulton, Maximilian Balandat, and Eytan Bakshy. Parallel bayesian optimization of multiple noisy objectives with expected hypervolume improvement. In *Advances in Neural Information Processing Systems*, volume 34, pp. 2187–2200, 2021.
- Peter I. Frazier. A tutorial on bayesian optimization. *arXiv preprint arXiv:1807.02811*, 2018.
- Yoav Freund and Robert E. Schapire. A decision-theoretic generalization of on-line learning and an application to boosting. *Journal of Computer and System Sciences*, 55(1):119–139, 1997.
- FunBO. FunBO: Discovering acquisition functions for bayesian optimization with funsearch. In *International Conference on Machine Learning*, 2025. URL <https://openreview.net/forum?id=XjbJR9374o>.
- Chuan Guo, Geoff Pleiss, Yu Sun, and Kilian Q. Weinberger. On calibration of modern neural networks. In *International Conference on Machine Learning*, pp. 1321–1330. PMLR, 2017.
- X. Ji et al. Adaptive feature-based low-rank compression of large language models via bayesian optimization. In *Findings of the Association for Computational Linguistics: EMNLP*, 2024. URL <https://dblp.dagstuhl.de/rec/conf/emnlp/JiXLYD0CZ24.html>.
- Donald R. Jones, Matthias Schonlau, and William J. Welch. Efficient global optimization of expensive black-box functions. *Journal of Global Optimization*, 13(4):455–492, 1998.
- Saurav Kadavath, Tom Conerly, Amanda Askell, Tom Henighan, Dawn Drain, Ethan Perez, Nicholas Schiefer, Zac Dodds, Nova DasSarma, Eli Tran-Johnson, Scott Johnston, Sheer El-Showk, Andy Jones, Nelson Elhage, Tristan Hume, Anna Chen, Yuntao Bai, Samuel R. Bowman, Stanislav Fort, Deep Ganguli, Danny Hernandez, Josh Jacobson, Jackson Kernion, Shauna Kravec, Liane Lovitt, Kamal Ndousse, Catherine Olsson, Sam Ringer, Dario Amodei, Tom Brown, Jack Clark, Nicholas Joseph, Ben Mann, Sam McCandlish, Chris Olah, and Jared Kaplan. Language models (mostly) know what they know. *arXiv preprint arXiv:2207.05221*, 2022.
- Joshua Knowles. ParEGO: A hybrid algorithm with on-line landscape approximation for expensive multiobjective optimization problems. In *IEEE Congress on Evolutionary Computation*, pp. 50–57. IEEE, 2006.
- LGBO. Unleashing llms in bayesian optimization: Preference-guided framework for scientific discovery. In *International Conference on Learning Representations*, 2026. URL <https://openreview.net/forum?id=LktUOZayG9>.
- Stephanie Lin, Jacob Hilton, and Owain Evans. Teaching models to express their uncertainty in words. *Transactions on Machine Learning Research*, 2022.
- Tennison Liu, Nicolás Astorga, Nabeel Seedat, and Mihaela van der Schaar. Large language models to enhance bayesian optimization. In *International Conference on Learning Representations*, 2024.
- Z. Liu et al. Maximizing intermediate checkpoint value in llm pretraining with bayesian optimization. In *International Conference on Machine Learning*, 2025. URL <https://proceedings.mlr.press/v267/liu25bv.html>.
- LMABO. Adaptive acquisition selection for bayesian optimization with large language models. In *International Conference on Learning Representations*, 2026. URL <https://openreview.net/forum?id=EPKmSgXvRe>.
- Model Fusion. Model fusion through bayesian optimization in language model fine-tuning. In *Advances in Neural Information Processing Systems*, 2024. URL [https://proceedings.neurips.cc/paper\\_files/paper/2024/file/34d3cf97696022b179171e5abda42c0b-Paper-Conference.pdf](https://proceedings.neurips.cc/paper_files/paper/2024/file/34d3cf97696022b179171e5abda42c0b-Paper-Conference.pdf).
- J. Schneider et al. Hyperband-based bayesian optimization for black-box prompt selection. In *International Conference on Machine Learning*, 2025. URL <https://proceedings.mlr.press/v267/schneider25b.html>.

## A ADDITIONAL EXPERIMENTAL DETAILS

**Candidate pools and objectives.** The molecule benchmarks are discrete candidate-pool optimization problems. ESOL uses a 100-molecule pool sampled from the MoleculeNet ESOL data, FreeSolv uses a 100-molecule pool sampled from MoleculeNet FreeSolv, and Lipophilicity uses a 150-molecule pool sampled from MoleculeNet Lipophilicity. RDKit descriptors are used as continuous features: molecular weight, logP, topological polar surface area, hydrogen-bond donors and acceptors, rotatable bonds, ring count, and QED. Each feature is min-max normalized within the candidate pool.

All reported molecule experiments optimize two normalized objectives. ESOL uses normalized measured log solubility and QED. FreeSolv uses normalized hydration favorability, defined as the negated experimental hydration free energy, and QED. Lipophilicity uses a windowed experimental lipophilicity score and QED. Prepared data files also include an RDKit logP-window objective for future experiments, but it is not used in the reported two-objective runs.

**LLM prior caches.** For each candidate, the LLM backend is queried once per expert role and the resulting prior file is cached. The BO loop then reads only the cache, so optimization comparisons are deterministic with respect to the same LLM prior data. Each cached record contains an expert name, objective-wise scores in  $[0, 1]$ , a scalar self-reported confidence value, and a free-text rationale. The molecule experiments use three expert roles per dataset, with one objective-specialized expert for each major objective and one balanced expert.

**Evaluation protocol.** All methods use the same initial-design size, budget, candidate pool, and seed set within each dataset. Hypervolume is computed on normalized maximization objectives with the origin as the reference point. We report final hypervolume, AUC hypervolume averaged over BO steps, and the best objective-sum value. Strong MOBO baselines use BoTorch implementations where available; residual-prior methods use the scalarized residual-UCB acquisition described in Section 4.

## B DERIVATIONS AND ALGORITHMIC DETAILS

### B.1 RESIDUAL-PRIOR BAYESIAN OPTIMIZATION

Let  $p_{j,t}(x)$  be the current LLM-derived prior for objective  $j$ . We model

$$f_j(x) = p_{j,t}(x) + r_j(x),$$

where  $r_j \sim \mathcal{GP}(0, k_j)$ . Given observations  $\mathcal{D}_t = \{(x_\tau, \mathbf{y}_\tau)\}_{\tau=1}^t$ , the residual targets are

$$\tilde{y}_{j,\tau} = y_{j,\tau} - p_{j,t}(x_\tau).$$

The GP posterior is fit to  $\{(x_\tau, \tilde{y}_{j,\tau})\}$ , yielding residual posterior mean  $m_{j,t}^r(x)$  and standard deviation  $s_{j,t}^r(x)$ . Therefore the predictive mean for the original objective is

$$\mathbb{E}[f_j(x) \mid \mathcal{D}_t] = p_{j,t}(x) + m_{j,t}^r(x).$$

This decomposition makes the LLM prior falsifiable: if the prior is wrong, the residual GP learns systematic corrections; if the prior is harmful, the counterfactual prior gate can reduce or drop it.

### B.2 REPUTATION-MARKET UPDATE

For expert  $e$  and objective  $j$ , define the scaled absolute error

$$\epsilon_{ej,t} = \frac{|\mu_{ej}(x_t) - y_{j,t}|}{s_{j,t}},$$

where  $s_{j,t}$  is a running objective scale. The reward

$$R_{ej,t} = \text{clip}(0.5 - 0.5\epsilon_{ej,t}^2, -2.0, 0.75)$$

is a shifted and clipped Gaussian log-score term. The shift allows accurate predictions to earn positive capital, while clipping prevents a single bad observation from dominating the market. Capital evolves as

$$K_{ej,t+1} = (1 - \lambda)K_{ej,t} + \eta \tilde{c}_{ej}(x_t)R_{ej,t}.$$

The expert weights are obtained by a temperature-controlled softmax over capital:

$$\alpha_{ej,t} = \frac{\exp(K_{ej,t}/T)}{\sum_{e'} \exp(K_{e'j,t}/T)}.$$

This is equivalent to a discounted exponential-weights update in capital space, with objective-specific experts competing within each objective.

### B.3 COUNTERFACTUAL PRIOR GATE

The prior gate compares three possible prior actions for each objective:

$$a \in \{\text{no\_conf}, \text{conf}, \text{drop}\}.$$

For each action, the historical residual sequence is

$$r_{j,\tau}^{(a)} = y_{j,\tau} - p_{j,t}^{(a)}(x_\tau).$$

The evidence score is the per-observation GP marginal log-likelihood

$$S_{j,t}(a) = \frac{1}{t} \log p(r_{j,1:t}^{(a)} \mid \mathcal{X}_t^{\text{obs}}).$$

The no-confidence action is used as the reference arm:

$$\ell_{j,t}(a) = \eta_p [S_{j,t}(a) - S_{j,t}(\text{no\_conf}) - \Delta_a].$$

With  $n_t$  observations and count-scale  $\kappa_0$ , the finite-data shrinkage factor is

$$\kappa_t = \sqrt{\frac{n_t}{n_t + \kappa_0}}.$$

The prior-gate policy is

$$\pi_{j,t}^p = (1 - \kappa_t) \mathbf{e}_{\text{no\_conf}} + \kappa_t \text{softmax}_a(\ell_{j,t}(a)).$$

Thus early rounds default toward the conservative no-confidence prior, while later rounds allow the GP evidence to select confidence weighting or prior abstention.

### B.4 COUNTERFACTUAL UPDATE GATE

The update gate decides whether confidence should scale future reputation rewards. The key observation is that the reputation market is deterministic once the reward history and confidence rule are fixed. We therefore maintain two parallel shadow markets at the beginning of round  $t$ :  $g = 0$  replays past expert rewards with confidence disabled, and  $g = 1$  replays the same rewards with reported confidence enabled.

Let  $K_{ej,t}^{(g)}$  denote the capital of expert  $e$  for objective  $j$  in shadow market  $g$ , after replaying observations up to round  $t - 1$ . The corresponding shadow expert weights are

$$\alpha_{ej,t}^{(g)} = \frac{\exp(K_{ej,t}^{(g)}/T)}{\sum_{e'} \exp(K_{e'j,t}^{(g)}/T)}.$$

Using these weights, each shadow market forms the same no-confidence/confidence/drop prior mixture as the main prior gate:

$$p_{j,t}^{(g)}(x) = \pi_{j,t}^p(\text{no\_conf}) p_{j,t}^{(g,\text{no\_conf})}(x) + \pi_{j,t}^p(\text{conf}) p_{j,t}^{(g,\text{conf})}(x),$$

where the drop-prior arm contributes zero. The nonzero component priors are

$$p_{j,t}^{(g,\text{no\_conf})}(x) = \frac{\sum_e \alpha_{ej,t}^{(g)} \mu_{ej}(x)}{\sum_e \alpha_{ej,t}^{(g)}}, \quad p_{j,t}^{(g,\text{conf})}(x) = \frac{\sum_e \alpha_{ej,t}^{(g)} c_{ej}(x) \mu_{ej}(x)}{\sum_e \alpha_{ej,t}^{(g)} c_{ej}(x)}.$$

After observing  $\mathbf{y}_t$ , the evaluated point  $x_t$  provides full-information feedback for both shadow markets:

$$L_{j,t}^u(g) = \frac{|y_{j,t} - p_{j,t}^{(g)}(x_t)|}{s_{j,t}}.$$

This loss asks a narrow counterfactual question: if previous reputation updates had followed rule  $g$ , would the resulting LLM prior have predicted the newly observed value more accurately?

The update-gate distribution follows Hedge:

$$\bar{L}_{j,t}^u(g) = L_{j,t}^u(g) - \frac{1}{2} \sum_{g' \in \{0,1\}} L_{j,t}^u(g'),$$

$$\pi_{j,t+1}^u(g) = \frac{\pi_{j,t}^u(g) \exp(-\eta_u \bar{L}_{j,t}^u(g))}{\sum_{g' \in \{0,1\}} \pi_{j,t}^u(g') \exp(-\eta_u \bar{L}_{j,t}^u(g'))}.$$

Centering the losses only subtracts an arm-independent constant within each objective and therefore does not change the softmax probabilities; it is used for numerical stability. The updated distribution  $\pi_{j,t+1}^u$  is used in future rounds.

For the real market update at round  $t$ , we deliberately use the pre-observation gate probability

$$\rho_{j,t} = \pi_{j,t}^u(1),$$

so that  $y_{j,t}$  is not used to decide how much confidence should scale its own reward. The resulting effective confidence multiplier is

$$\tilde{c}_{ej,t}^u = 1 + \rho_{j,t}(c_{ej}(x_t) - 1),$$

and the real capital update is

$$K_{ej,t+1} = \text{clip}((1 - \lambda)K_{ej,t} + \eta \tilde{c}_{ej,t}^u R_{ej,t}, K_{\min}, K_{\max}).$$

Here  $K_{\min}$  and  $K_{\max}$  are fixed clipping bounds that prevent a single update from making expert capital numerically dominant.

The same observation is then replayed into both shadow markets. Define the shadow confidence multiplier

$$\omega_{ej,t}^{(0)} = 1, \quad \omega_{ej,t}^{(1)} = c_{ej}(x_t).$$

With the reputation reward  $R_{ej,t}$  from the observed prediction error, the two shadow markets evolve as

$$K_{ej,t+1}^{(g)} = \text{clip}((1 - \lambda)K_{ej,t}^{(g)} + \eta \omega_{ej,t}^{(g)} R_{ej,t}, K_{\min}, K_{\max}), \quad g \in \{0, 1\}.$$

Thus the newly observed point affects the real market through the old gate  $\rho_{j,t}$ , while it affects the next gate only through the shadow-market losses and replay updates. Unlike a bandit meta-gate, this procedure observes the counterfactual loss of both update arms at every step and learns from an endogenous replay signal rather than from delayed, high-variance downstream hypervolume changes.

## C PSEUDOCODE

**Algorithm 1: CF-V2 Evidence-Gated LLM Prior BO**  
**Input:** candidate pool  $\mathcal{X}$ , cached expert priors  $\mu_{ej}(x)$ , confidences  $c_{ej}(x)$ , initial design size  $n_0$ , budget  $B$ .  
**Initialize:** evaluate  $n_0$  candidates to form  $\mathcal{D}_{n_0}$  and  $\mathcal{X}_{n_0}^{\text{obs}}$ ; initialize expert-objective capital  $K_{ej}$ , prior-gate policy  $\pi_j^p$ , update-gate policy  $\pi_j^u$ , and shadow markets  $K^{(0)}, K^{(1)}$ .

1. For  $t = n_0, \dots, B - 1$ , compute  $\epsilon_{ej,t}$  and  $R_{ej,t}$  from the newest observation.
2. Update the actual reputation market using the pre-observation update gate  $\rho_{j,t} = \pi_{j,t}^u(1)$ .
3. Score both update-gate shadow markets at  $x_t$ , update  $\pi_j^u$  by full-information Hedge, and replay the observation into both shadows.
4. For each objective  $j$ , score the no-confidence, confidence, and drop-prior residual histories by fixed-kernel GP marginal likelihood; update  $\pi_j^p$ .
5. Aggregate  $p_{j,t}(x)$  with the three-arm prior mixture and fit residual GP surrogates to  $y_{j,\tau} - p_{j,t}(x_\tau)$ .
6. Select  $x_{t+1} = \arg \max_{x \in \mathcal{X} \setminus \mathcal{X}_t^{\text{obs}}} A_t(x)$ , evaluate it, and append  $x_{t+1}$  and  $(x_{t+1}, \mathbf{y}_{t+1})$  to form  $\mathcal{X}_{t+1}^{\text{obs}}$  and  $\mathcal{D}_{t+1}$ .

**Output:** evaluated candidates and the final non-dominated set.

Figure 7: Pseudocode for the fixed CF-V2 method used in the main experiments.

## D HYPERPARAMETER SENSITIVITY

The main method intentionally fixes a compact hyperparameter set. We nevertheless include sensitivity diagnostics for the two most important counterfactual-gate parameters: the prior-abstention margin  $\Delta_{\text{drop}}$  and the prior-gate inverse temperature  $\eta_p$ .

The sensitivity results support two conclusions. First, the drop margin interacts with the LLM backend: Qwen3.6-Flash prefers a more aggressive abstention margin in the collected runs, while Qwen3.7-Max and DeepSeek-V4-Pro are less aligned with that choice. Second, sharpening the prior-gate temperature does not consistently improve performance. This explains why we avoid treating the margin portfolio as the main method: one-step prior fit is not sufficient to choose the best exploration behavior.

Table 9: Drop-margin sensitivity on ESOL across LLM backends. Values are final hypervolume; missing cells indicate runs not collected.

Backend	$\Delta_{\text{drop}} = 0.05$	$\Delta_{\text{drop}} = 0.25$	$\Delta_{\text{drop}} = 1.0$
Qwen3.6-Flash	0.7561	0.7480	0.7515
Qwen3.7-Max	0.7470	0.7445	0.7507
DeepSeek-V4-Pro	0.7515	—	0.7500

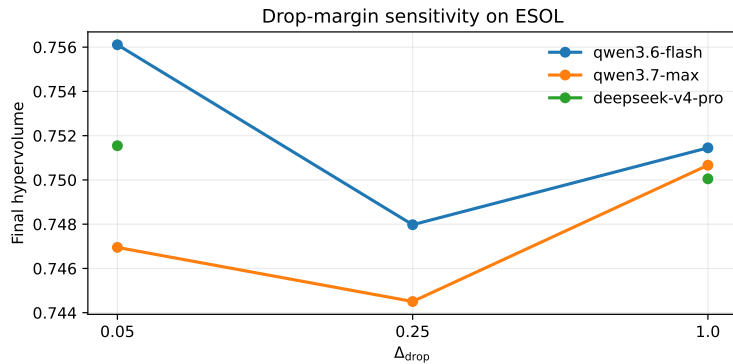


Figure 8: Drop-margin sensitivity on ESOL across three LLM backends. The best margin differs across backends, which motivates our decision to keep a fixed, transparent margin in the main method and treat automatic margin selection as future work.

Table 10: Prior-gate temperature sensitivity. Values are final hypervolume for  $\eta_p = 1$  and a sharper  $\eta_p = 8$  gate.

Setting	$\eta_p = 1$	$\eta_p = 8$
ESOL / Qwen3.6-Flash	0.7561	0.7416
Synthetic / overconfident bad	0.4788	0.4791
Synthetic / correlated bad experts	0.4461	0.4461